

# Compact slot antenna with enhanced band-edge selectivity and switchable band-notched functions for UWB applications

ISSN 1751-8725

Received on 26th September 2018

Revised 14th February 2019

Accepted on 18th February 2019

doi: 10.1049/iet-map.2018.5832

www.ietdl.org

Hailong Yang<sup>1</sup>, Xiaoli Xi<sup>1,2</sup> ✉, Yuchen Zhao<sup>1</sup>, Yumeng Tan<sup>1</sup>, Yanning Yuan<sup>1</sup>, Lili Wang<sup>1</sup>

<sup>1</sup>Faculty of Automation and Information Engineering, Xi'an University of Technology, Xi'an 710048, People's Republic of China

<sup>2</sup>Science and Technology on High Power Microwave Laboratory, Northwest Institute of Nuclear Technology, Xi'an 710024, People's Republic of China

✉ E-mail: xixiaoli@xaut.edu.cn

**Abstract:** In this study, a new reconfigurable stepped slot antenna with enhanced band-edge selectivity of the UWB passband and switchable band-notched characteristic is presented. Good out-of-band rejection and sharp cut-off at band-edge are achieved by the use of defected ground structure (DGS) and a parasitic slot near the stepped slot. The well-designed DGS not only produces transmission zero to obtain good cut-off property in upper sideband but also provides better impedance matching of in-band. The frequency range of the proposed antenna is from 3.1 to 11.1 GHz (114%) with the reflection coefficient  $< -10$  dB. The shape factor is 1.05, which indicates that the proposed design has an excellent selectivity. To obtain the notched band, two passive strip lines near the feeding line are designed. Furthermore, the reconfigurable function with four states can be easily realised by the control of two diodes between the passive strip line and the ground. The structures of the notched band and bias circuit are relatively simple and independent of antenna radiation structure. The performance of the antenna is presented and compared with other competitive antennas. The proposed design has many significant advantages in dimension, good out-of-band characteristics, and controllable states for different UWB applications.

## 1 Introduction

Ultra-wideband (UWB) communication system has achieved an unprecedented improvement since the FCC in the USA designated the 3.1–10.6 GHz operation band for commercial applications [1]. As a key part of the RF front-end in the UWB system, antennas and filters are usually studied and designed as two separate devices [2]. Due to the wide operating band of the UWB system (3.1–10.6 GHz), UWB systems are vulnerable to interference from narrowband signals in the UWB band and other wireless communication systems out of band. The unwanted in-band and out-of-band signals will cause electromagnetic interference on the UWB system. Usually, we avoid the out-of-band interference signals and improve the selectivity of the UWB system by designing a filter with bandpass characteristics at the end of the antenna. However, this method increases the dimension and costs of RF front-end in the UWB system and leads to the loss of insertion between the antenna and filter. [2, 3] Hence, it is a valuable point to propose a filtering UWB antenna to improve the RF front-end performance with compact size and low cost.

Many UWB antennas with good performance have been reported in [3–8]. It is found that the authors are more concerned to the size of structure [3, 4], bandwidth [5, 6], and radiation characteristics of the antenna [7, 8], but little attention is paid to the sideband selection characteristics of antennas and the suppression of out-of-band systems. In [9], an impulse UWB design with good bandpass characteristics is obtained by etching a bandpass filter on the feeding line. However, the filter characteristics of the design are not discussed in detail in the article. The dimension of the design is about  $35 \times 34$  mm. By cascading the feeding line with bandpass filter function with the radiation patch, integrated filter antennas [10, 11] with improved band-edge selectivity are achieved. However, cascaded filter and radiation patch will inevitably increase the size of antenna. The demotions the filter antennas are  $53 \times 22$  [10] and  $53 \times 42$  mm [11], which are bigger than most UWB antennas in [1–9]. In [12], a slot UWB antenna with good band-edge selectivity using stepped impedance resonator feeding line is proposed. Although it plays a key role in improving the upper band-edge selectivity, the low-pass feeding line has a negative effect on radiation efficiency. The radiation efficiency of

the referenced antenna in [12] was about 80%. Also, the impedance characteristics in the UWB band are not ideal, and the reflection coefficient of the proposed design is only  $-10$  dB.

To overcome some system signals in the UWB band such as the WiMAX and WLAN operating in the 3.3–3.6, and 5.15–5.825 GHz [5, 6], various notched band techniques are applied in operating band to reject the unwanted signals. The most common techniques were etching various slots on the radiating patch [5, 6, 13, 14] or the ground plane [15, 16], or adding parasitic structure near the feeding line [17–19]. However, all these notch approaches are used for suppressing the changeless band of interference signals. No matter whether the interference band exists or not, the notch function is always in operation. In order to solve these problems, several designs with reconfigurable characteristics have been reported [20–22]. When multiple functions are implemented on an antenna through the reconfigurable structures and switches, the reconfigurable antenna becomes more efficient and cost-effective. In [20], band notch characteristics are achieved by etching two modified slots in the radiating patch. Reconfigurability is obtained by controlling the bias statuses of the switches along the slots. In [21], the reconfigurable structure is achieved by adding a PIN diode on the  $\pi$ -shaped slot. When the PIN diode is turned on, the  $\pi$ -shaped slot is divided into two C-shaped slots, and a new resonance frequency is generated at 5–6 GHz. In [22], a reconfigurable UWB antenna with switchable dual band-notches is designed. Three different states at UWB, or the antenna with notched frequencies at WiMAX or WLAN band could be obtained by using five PIN diodes. In [23], a stepped slot antenna with reconfigurable is proposed, due to the loss on the feed microstrip line, the antenna exhibits poor impedance characteristics. In [24], a small slot antenna with switchable frequency bands is designed. Total four switchable states in communicating are designed by the employ of multiple PIN diodes, i.e. 2.8–10.7 GHz in UWB band, 3.2–4.5, 4.3–7.8, and 7.9–11.2 GHz. The improved design of the ladder slot is beneficial to the improvement of the impedance in the slot antenna band and the design of the reconfigurable structure. However, the reconfigurable structure and bias circuit on the radiation patch will have more influence on the antenna.

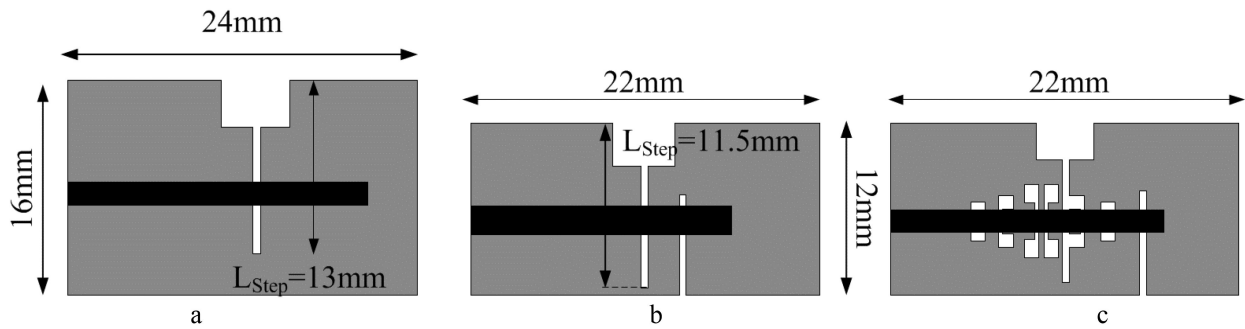


**Fig. 1** Development of the proposed design  
(a) Antenna 1, (b) Antenna 2, (c) Antenna 3

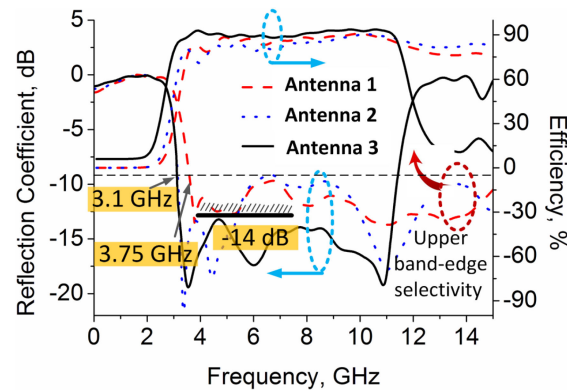


**Fig. 2** Radiation efficiency and Reflection coefficient curves comparison of three antennas shown in Fig. 1

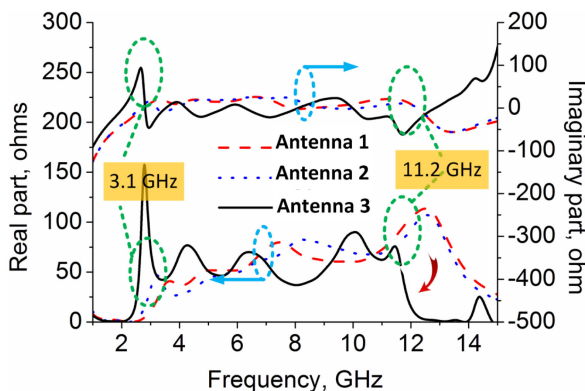


**Fig. 3** Simulated input impedance curves comparison of three antennas shown in Fig. 1

Inspired by the referenced antenna in [25], a compact reconfigurable UWB slot antenna with enhanced band-edge selectivity and switchable band-notched functions is presented. First, a modified slot with defected ground structure (DGS) is proposed. The well-designed DGS not only produces transmission zero to obtain good cut-off property in upper sideband but also provides better in-band impedance matching. Second, by the addition of a parasitic slot near the stepped slot, the operating band and the characteristics of frequency selection at low frequency have also been improved [12]. What's more, to filter out some wireless communication systems in the UWB band, such as WLAN and WiMAX, two microstrip lines and feeding line are placed in parallel. (Total four configurations could be achieved from the parallel strips and the ground shorting with PIN diodes.) The bias circuit is simple and independent, which will reduce the complexity of the antenna and the influence of the bias circuit on the antenna. The dimension of the proposed design is  $22 \times 12 \text{ mm}^2$ , which is more compact than most of antennas reported in [3–23]. The shape factor of the proposed antenna is 1.05, which is very close to the 1. Compared with the referenced antennas in [9–11], the shape factor of the antenna in this study has improved by 6, 4, and 4%, respectively. Moreover, the bias circuit and the notch

structure are not directly connected to the radiation patch, which does not affect the overall dimension and performance of the antenna. Compared with the slot antenna in [12], the proposed design with reconfigurable function has many controllable states for different UWB applications.

## 2 Antenna design and performance

### 2.1 UWB antenna with improved band-edge selectivity

The development of the presented design is illustrated in Fig. 1. Fig. 1a exhibits the prototype of the design, named antenna 1. The size of the antenna 1 is  $24 \times 16 \text{ mm}^2$ . The design is fabricated on an RO-5880 substrate with dielectric constant  $\epsilon_r = 2.2$  and height of 0.787 mm. Several resonant frequencies and UWB functions are realised by using  $50 \Omega$  microstrip feeding line to excite the slot embedded at the centre of the ground plane [12]. The simulated reflection coefficient is shown in Fig. 2. It can be observed in Fig. 3 that the antenna 1 has poor selectivity in the high-frequency band, and the start frequency of the passband bandwidth is 3.75 GHz, which does not satisfy the needs of the UWB with a low operating band of 3.1 GHz. As we all know that the length of the slot and the dimension of the antenna have a decisive effect on the first resonant frequency [12]. Therefore, for the slot antenna, the lower resonant frequency means a longer stepped slot length. However, the length of the slot of the antenna is difficult to increase due to the smaller size of the antenna. To solve the problems mentioned above, a paralleled slot close to the radiation slot is added [12]. The start resonance frequency could be effectively decreased and a new reflection zero near the band-edge is generated. In this way, the antenna 2 is designed with small size ( $22 \times 12 \text{ mm}^2$ ), as illustrated in Fig. 1b. From what we can see in Fig. 2, the lower initial frequency is also developed by decreasing from 3.75 to 3.1 GHz.

As shown in Fig. 2, although the selectivity and bandwidth of the low-frequency band have been improved, the selectivity of the upper band has not been improved. In order to improve selectivity at high frequencies, the modified stepped slot with three pairs of DGS structure is designed. The DGS structure can be seen as a filter, it can generate resonant frequency and stop band characteristics in corresponding frequency band. [24, 25]. Then,

the problem that the antenna size increases and the low radiation efficiency caused by filter-fed microstrip line can be avoided by the use of modified stepped slot with DGS. In [24], three pairs of DGS structures are studied and applied to create the transmission zero in the high-frequency band, which can improve the selectivity of upper band. Therefore, three pairs of DGS structures with different size are co-designed with stepped slot, as seen in Fig. 1c. As shown in Fig. 2, the impedance and sideband selectivity of antenna 3 are improved by using modified stepped slot with DGS structure. The maximum reflection coefficient of antenna 3 is 14 dB, which is about 40% higher than that of antenna 1 and antenna 2. In addition, the simulated radiation efficiency of the proposed design with DGS is about 90%, which is about 12.5% higher than the antenna in our previous design [12]. This is because the improved stepped slot can have more resonant modes, which is beneficial to the improvement of the in-band impedance. At the same time, the improvement of the in-band impedance characteristics is beneficial to the improvement of the radiation efficiency. The DGS structure can avoid the problem of poor impedance characteristics and low radiation efficiency caused by stepped feed microstrip line in [12]. Compared with the design in [12], the antenna in this study not only has good band-edge selectivity, but also has improved in-band impedance and radiation efficiency. In addition, this paper will

discuss the in-band notch and reconfigurable structure of the antenna in the following sections. This is conducive to further improvement of slot antennas.

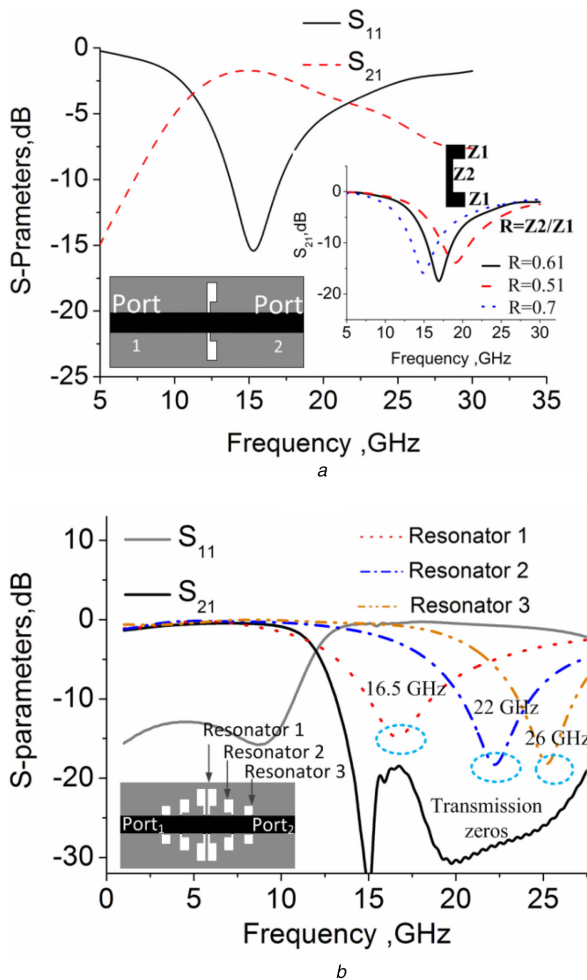
To better understand the improved selectivity of the proposed design, the corresponding input impedance curves are also given in Fig. 3. It is observed that the characteristics of both the imaginary and real parts of the design in the upper and lower frequency of the passband have changed sharply after the narrow-band slot and DGS type are added. Eventually, this steep change of impedance produces a steep change of reflection coefficient and gain. Then, this steeply varying impedance produces a highly selective reflection coefficient and gain in the side bands.

Fig. 4a shows the schematic view and simulated S-parameter of the DGS unit. In order to further obtain the different performance of the DGS, the DGS units with different impedance ratio are also studied as shown in Fig. 4a. The simulated results show that each DGS unit designed in the ground plane of the design can generate stop band and transmission zero characteristics at the corresponding resonant frequency. The corresponding resonant can be shifted by the adjusting the impedance ratio of DGS. Transmission zeros built at upper stop band is favourable for obtaining good band-edge selectivity and harmonic suppression [26]. As seen in Fig. 4b, three pairs of DGS with different dimensions are proposed to achieve wide upper stop band. The simulated transmission zeros of three different DGS resonators are 16.5, 22, and 26 GHz, respectively.

Table 1 shows the comparison of antenna parameters before and after improvement. It is clear from Table 1 that the dimensions, impedance of in the UWB band, bandwidth, and selectivity of antenna 3 have been significantly improved.

## 2.2 Antenna with reconfigurable band-notched characteristics

Fig. 5a shows an improved final design of reconfigurable filtering antenna. In order to achieve notch function, two parasitic microstrip lines near the feeding line are designed. The coupled current flows through the parasitic microstrip line with a short circuit to the ground plane. The notched band of the design is related to the length of the current path, as seen in Fig. 6. It can be seen from the diagram that the longer the current path, the lower the resonance frequency [12]. The length of the current path is about  $\lambda/4$  of the corresponding frequency. The adjustable frequency range is 3.2–6 GHz, which includes the interference bands of WiMAX and WLAN. Therefore, the reconfigurable function of antenna can be easily realised by replacing short circuit with two PIN diodes. The equivalent circuit of the PIN diode is shown in Fig. 5b. BAR64-02 V PIN diode model is selected, which is applied to connect the microstrip line and the ground plane. To active the diode, a DC forward voltage (VF) of 1.8 V is used. To provide RF isolation and limit the DC current the inductors and resistors of 22 nH and 100  $\Omega$  are used in the circuit. Four states of the proposed design are summarised in Table 2. The corresponding reflection coefficients and the surface currents of the proposed design with different states are presented in Fig. 7. It is found in Fig. 7a that when the two diodes are off (in state I), the current mainly concentrates near the step slot and parasitic strip slot. The current is concentrated near the stepped slots and the DGS, which means that the stepped slot is strongly coupled with the DGS resonators and resonating on desired operating band. The optimal operating band of the antenna is 3.1–11 GHz, which shows good band-edge selectivity. In addition, the phenomenon of the current distribution demonstrates that when the two diodes are all off, the notch structure has almost no effect on the bandwidth and shape factor of the antenna operating in state I. In state II, state III, and



**Fig. 4** S-parameters of DGS  
(a) Reflection coefficient of DGS unit. (S<sub>21</sub> varies with the impedance ratio of DGS cell), (b) The transmission zeros of three DGS units with different sizes and the S-parameters of DGS

**Table 1** Comparison of antenna parameters before and after improvement

Antenna	$\epsilon_r$	Size, mm <sup>2</sup>	$L_{Step}$ , mm	-10 dB bandwidth, GHz	Maximum reflection coefficient of in-band, dB	Shape factor, K
antenna 1	2.2	24 × 16 = 384	13	3.75–15	-10	(>1.64)
antenna 2	2.2	24 × 12 = 288	11	3.5–11	-9.7	(1.09)
antenna 3	2.2	24 × 12 = 288	11	3.1–11.1	-14	(1.05)

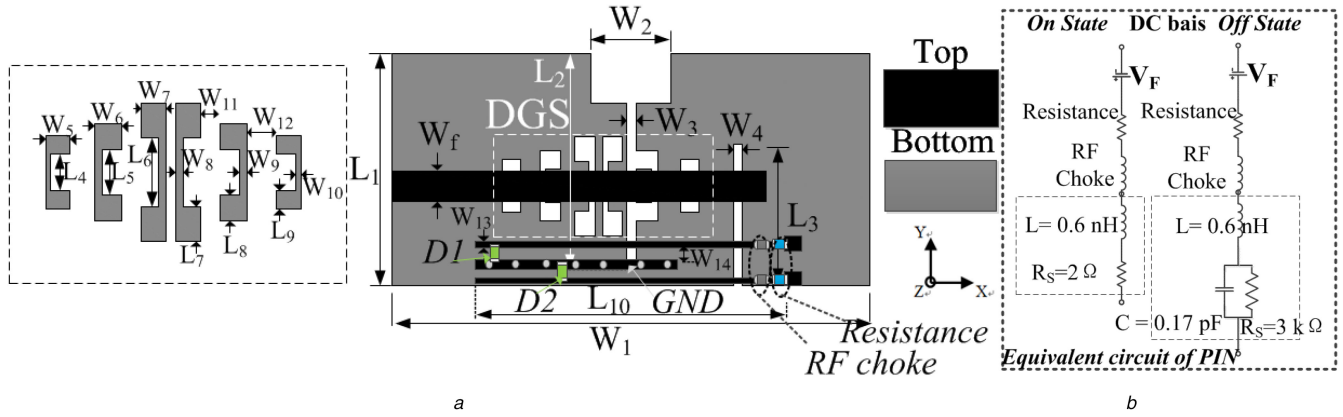


**Fig. 5** Proposed antenna  
(a) Geometry of the antenna, (b) Equivalent circuit of the PIN diode

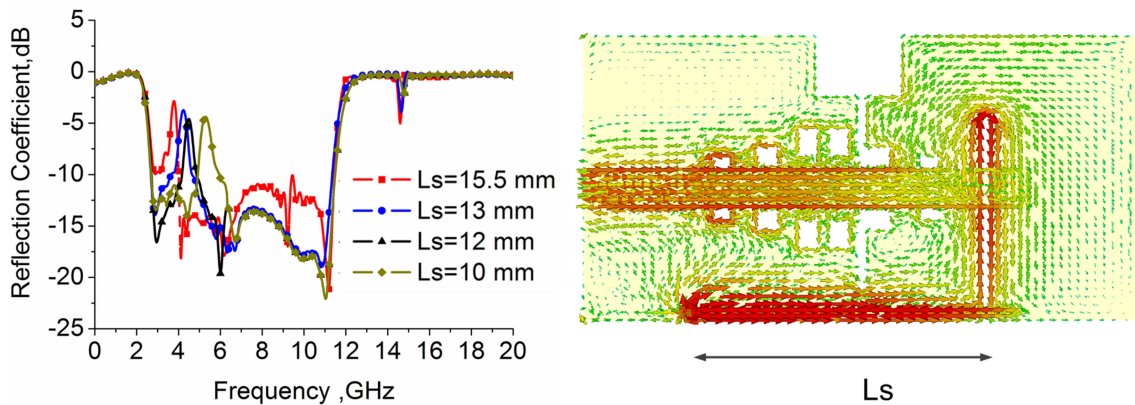


**Fig. 6** *S*-parameters of the presented design with various current path  $L_s$  ( $L_s$  is the path length of the current, which can be regulated by the position of the PIN diode)

**Table 2** Various states of the reconfigurable slot antenna

State	D1	D2	Characteristics
state I	off	off	UWB (3.1–11.1 GHz)
state II	on	off	antenna with band-notched function at 3.5 GHz(WiMAX)
state III	off	on	antenna with band-notched function at 5.5 GHz(WLAN)
state IV	on	on	antenna with band-notched function at 3.5 and 5.5 GHz(WiMAX and WLAN)

state IV, Figs. 7(b–d), current is mostly flowing in parasitic strip line which confirm their stop band behaviour at corresponding frequencies. It is clearly shown that the simple and independent biasing circuit of the PIN diodes has little effect on the bandwidth and band-edge selectivity of the proposed design.

The proposed antenna is simulated by the adoption of commercially software CST microwave studio. The values of the optimised design are fabricated and shown in Table 3.

### 3 Results and discussion

To analyse the performance of the final design, the proposed design is fabricated and measured. This section introduces and discusses several simulations and test results of the design, including frequency domain analysis and time-domain analysis.

#### 3.1 Frequency domain analysis

The fabricated slot antenna with a DC bias circuit is shown in Fig. 8. The bias lines and diodes cathode were isolated from the induced RF signal on the ground plane using 22 nH inductors. The 100  $\Omega$  limiting current resistances were used during measurements. The frequency responses of the simulated and measured reflection coefficient in four states of the reconfigurable slot antenna are shown in Fig. 9. Measured results show good agreement with the simulated results. As seen in Fig. 9a, when the antenna operates in

state I, the operating band with  $-10$  dB reflection coefficient is from 3.1 to 11.1 GHz. Good bandpass filtering performance is obtained, the shape factor of the proposed antenna is 1.05. It can also be observed that the design has good in-band impedance matching and achieves a reflection coefficient of  $-14$  dB. Figs. 9b–d show the reflection coefficients of the diode in the gated state and the antenna in state II, state III, and state IV. The measured results are agreed well with the simulated results. By controlling the pin diode, the proposed design shows good in-band and out-of-band filtering characteristics.

Fig. 10 illustrates the measured and simulated gain and efficiency of the proposed design in four states. As seen in Fig. 10a, the simulated and measured peak gain in the operating band is about 1.3–4 dBi, the simulated and measured efficiency are  $>85\%$  in the entire passband. Both gain and radiation efficiency of the proposed design exhibit good sideband selection characteristics. Figs. 10b–d show the measured and simulated gain and efficiency of the proposed design with the notched bands, the gain and efficiency are significantly reduced to  $-4$  dBi and 50% at notch frequency, respectively.

To further understand the characteristics of band-edge selectivity and band-notched function of the proposed design, the simulated input impedance characteristics of the antenna in state IV with band notch characteristics at 3.5 and 5.5 GHz are proposed in Fig. 11. It can be seen in Fig. 11 that the real and imaginary parts of

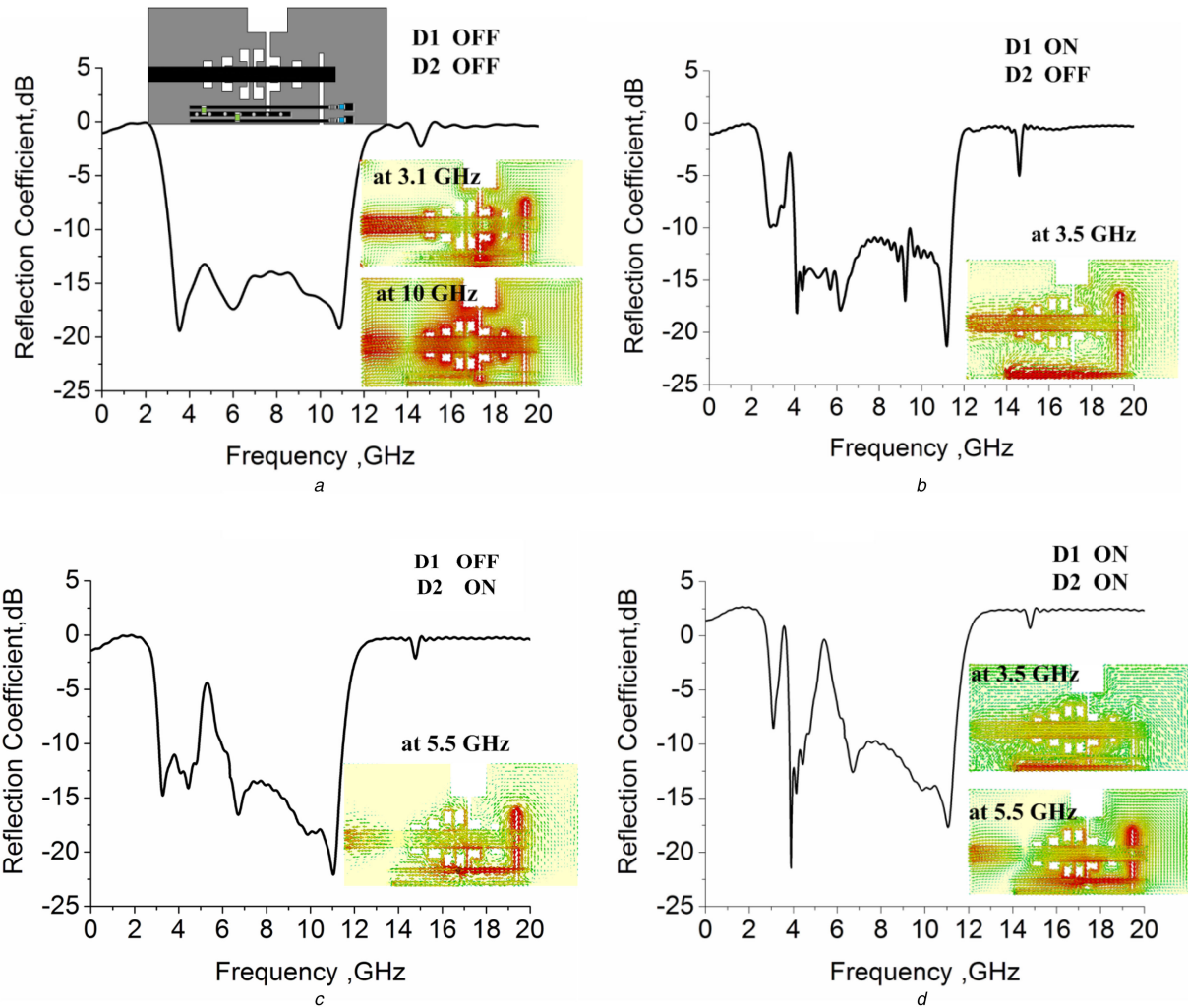


**Fig. 7** *S*-parameter and the surface current distributions of the proposed design in different states  
 (a) State I, (b) State II, (c) State III, (d) State IV

**Table 3** Dimensions of the proposed design

Parameters	$L_1$	$L_2$	$L_3$	$L_4$	$L_5$	$L_6$	$L_7$	$L_8$	$L_9$	$L_{10}$	$W_1$	$W_2$	$W_3$
value, mm	22	11.5	9	1.6	2	3	1.5	1.1	0.8	16	12	4.2	0.5
Parameters	$W_4$	$W_5$	$W_6$	$W_7$	$W_8$	$W_9$	$W_{10}$	$W_{11}$	$W_{12}$	$W_{13}$	$W_{14}$	$W_f$	—
value, mm	0.5	1	1.2	1	0.3	0.2	0.2	1	2	0.3	0.6	2	—

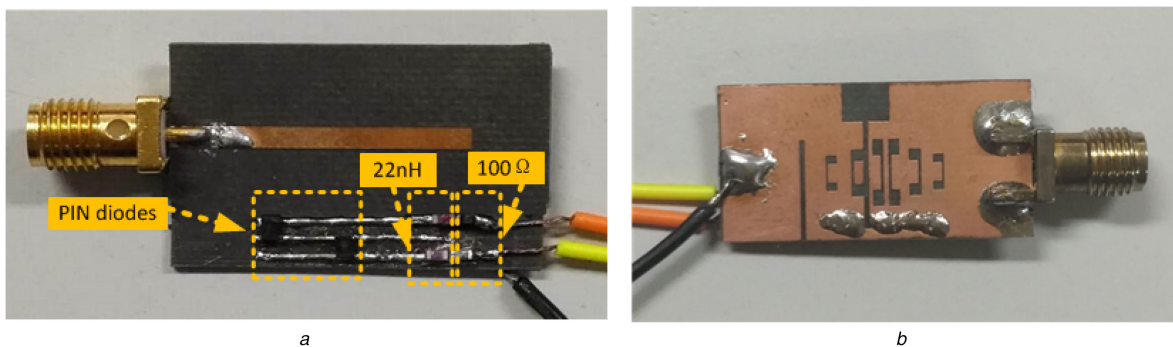


**Fig. 8** Photograph of the design  
 (a) Top, (b) Bottom

the simulation are relatively flat in the entire bandwidth of UWB band, in which the real part of the design is tends to 50 ohms and the imaginary part is approximates to 0. As shown in Fig. 11, the impedance of the band-edge and notched bands decreases rapidly in both the real and imaginary parts, and exhibits significant changes. Then, the good band-edge selectivity and band-notched

characteristics of the proposed antenna are obtained due to the band impedance mismatching at band-edge and notched band.

The normalised radiation patterns of the proposed design in state I mode at 3.1, 6, and 10 GHz are plotted in Fig. 12. In order to better understand the radiation, 3-D radiation patterns at 3.1 and 10 GHz and cross-polarisation at 6 GHz are also added. It is obvious that the measured radiation patterns in H planes are agreed

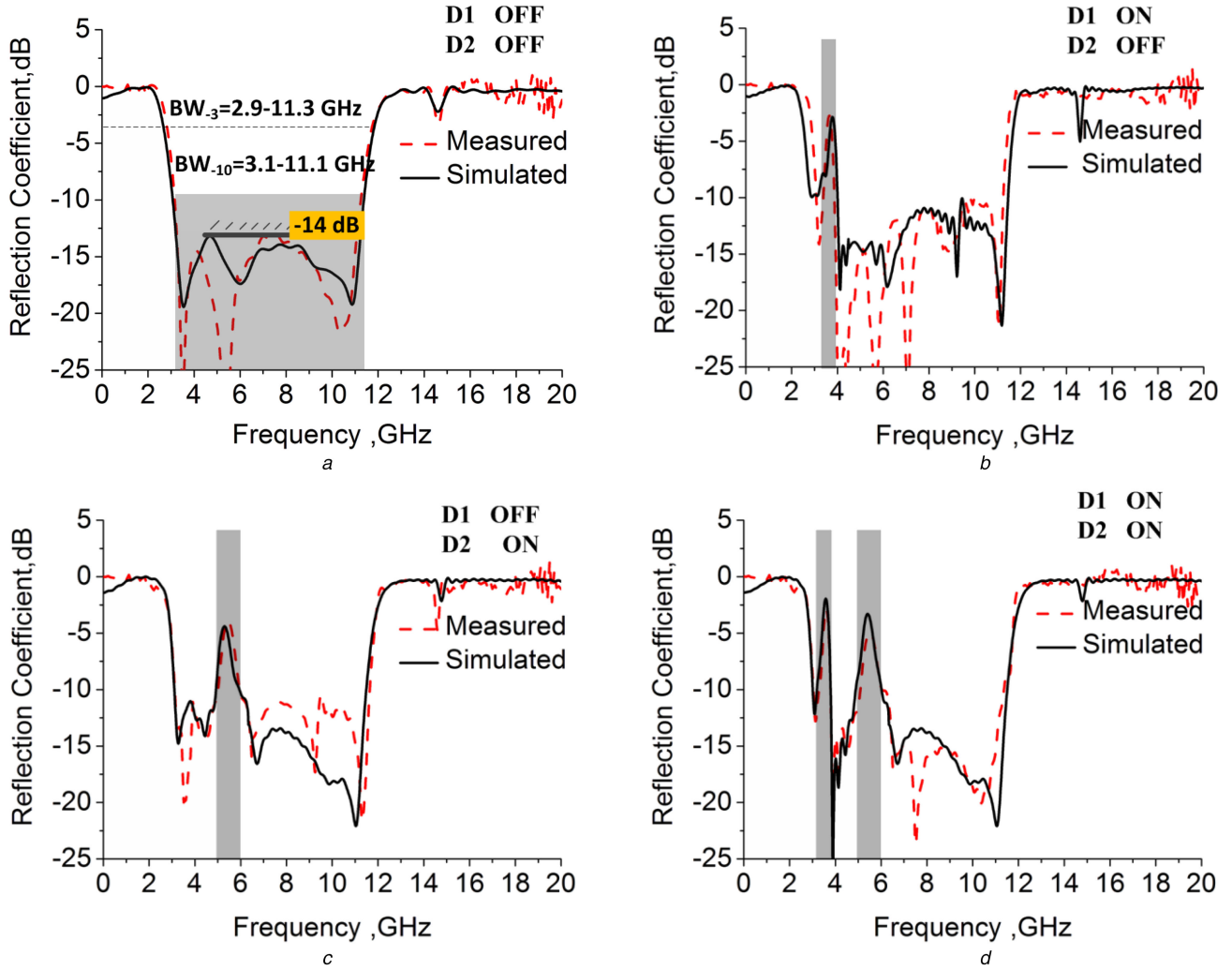


**Fig. 9** *S*-parameters of the proposed design in four states  
(a) State I, (b) State II, (c) State III, (d) State IV

well with the simulated results and show quasi-omnidirectional radiation pattern in operating frequencies. However, there have certain directional characteristics in E-plane at 10 GHz, which are mainly due to the imbalance of current distribution at higher frequencies. As shown in Fig. 12b, the cross-polarisation average value is  $-15$  dB at 6 GHz, which show good cross-polar radiation. The experimental results show that the antenna performs well in the filtering the interference signals in the UWB band and out-of-band in the frequency domain.

### 3.2 Time-domain analysis

The UWB antenna is used to transmit time-domain pulse signals, it is also important to discuss the time-domain characteristics of the proposed design. In order to discuss both in-band and out-band time-domain characteristics, two identical antennas in state IV are selected.

The measured group delay of the proposed design in state IV is shown in Fig. 13. Two identical antennas are placed face-to-face at a distance of 50 cm. It is observed that the variation of the antenna in state IV is  $<0.5$  ns across the entire bandwidth of UWB band except at the notched band, which indicates that the antenna has good linear transmission characteristics. It can also be observed that the antenna has a large group delay both in the sideband and out of the band, which is in sharp contrast to the in-band signal group delay. The measured result confirms that the good in-band and out-of-band filtering characteristics can also be demonstrated through the group delay of the antenna.

Fig. 14 shows the transfer function for two identical antennas with the distance of 50 cm. It can be seen in Fig. 14a that the transmission function amplitude of the antenna decreases rapidly in

notch band and band-edge and has a better stability in band. The phase of the transmission function of the transceiver antenna group is basically linear in the whole bandwidth except for notched bands.

The input and received waveforms of the antenna are shown in Fig. 15. Two identical antennas are placed face-to-face and edge-to-side, respectively. One antenna is used as the transmitting antenna to excite a time-domain pulse signal and then the other antenna receives a time-domain pulse signal after a certain time delay. In order to satisfy the transmission power limit prescribed by FCC for UWB system [27], the fifth-order Gauss pulse signal is used as an excitation signal whose signal expression is given by (1)

$$s_i(t) = GM_s(t) = C \left( -\frac{t^5}{\sqrt{2\pi}\sigma^{11}} + \frac{10t^3}{\sqrt{2\pi}\sigma^9} - \frac{15t}{\sqrt{2\pi}\sigma^7} \right) \times \exp\left(-\frac{t^2}{2\sigma^2}\right) \quad (1)$$

where,  $\sigma = 51$  ps, the constant  $C$  can be used to select the appropriate amplitude to make the pulse signal conform to the FCC radiation power spectrum. The time-domain waveform of the fifth-order Gauss pulse signal is presented in Fig. 15. It is found that when the two diodes  $D1$  and  $D2$  are on (in state IV), the received signal of the antenna in both two cases (face-to-face and side-to-side) will produce ringing distortion, but when the PIN diodes  $D1$  and  $D2$  are off (in state I) will not. It is because of the poor impedance characteristics of the antenna in notched band. It can also be found that when the two diodes are in the off state, the waveforms of the input and received signals are very close, which indicates that the signal is less affected in the process of receiving

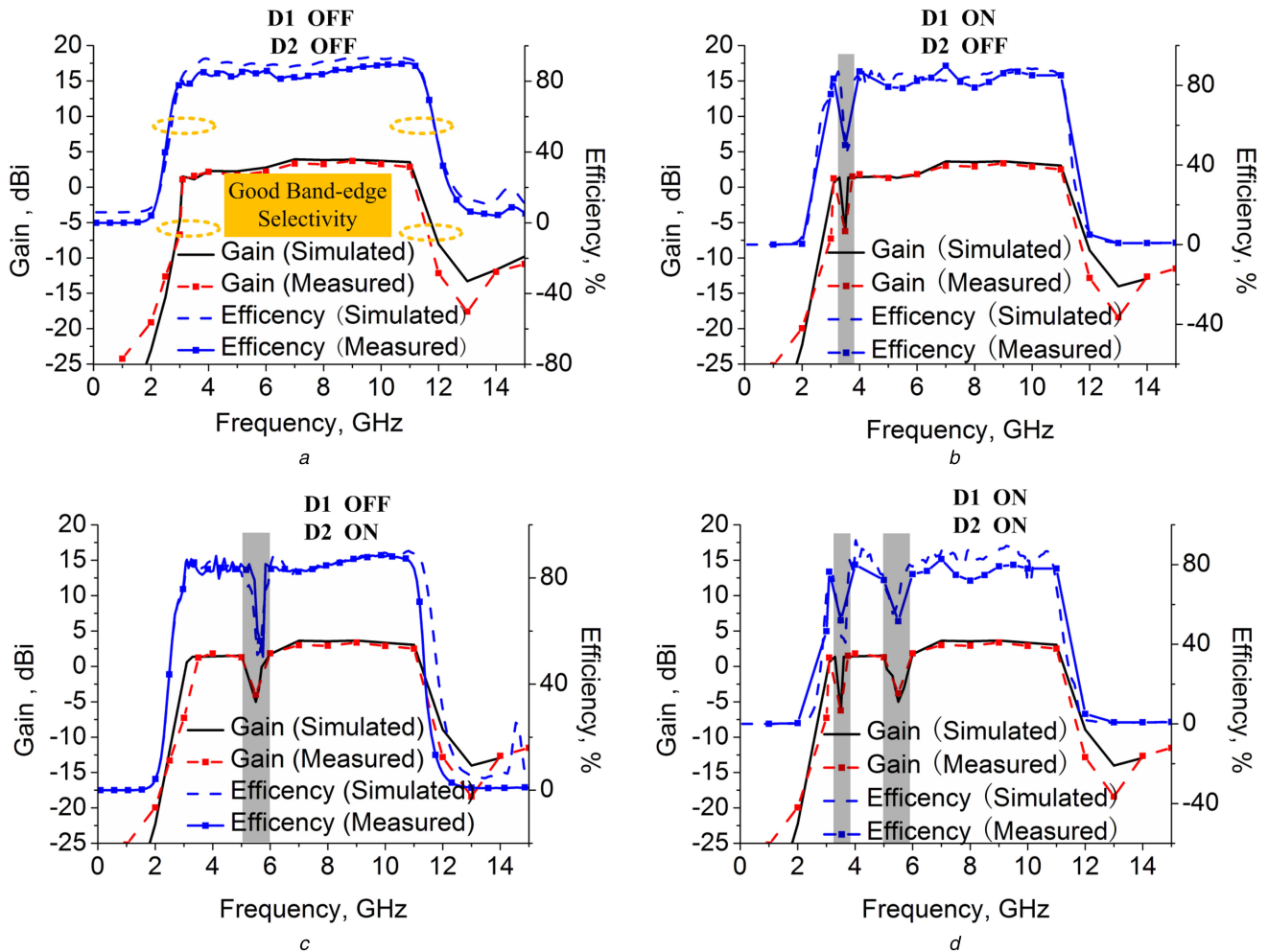


**Fig. 10** Gain and efficiency of the proposed design in four states (a) State I, (b) State II, (c) State III, (d) State IV

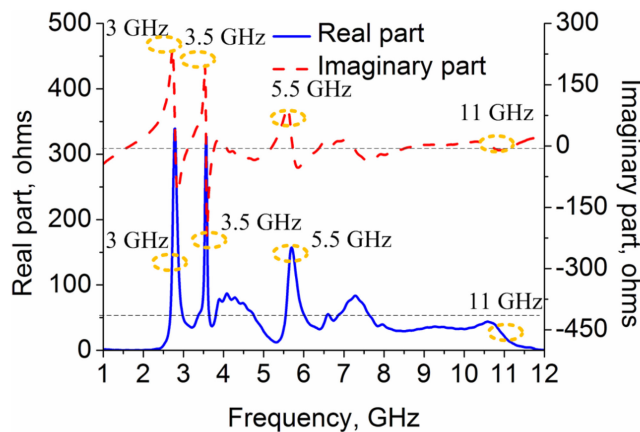


**Fig. 11** Input impedances of the proposed antenna in state IV with dual band-notched characteristics

and transmitting. The proposed antenna exhibits good time-domain characteristics.

#### 4 Conclusion

In this design, a compact reconfigurable slot antenna with bandpass filter characteristics and switchable band-notched function is presented. By etching the DGS and parasitic slot, both the upper and lower selectivity in the passband of the proposed design are improved and good filtering function is obtained. To reject the unwanted signals in the UWB band, two passive strip lines close to the feed microstrip line are applied. The reconfigurable structure of the design is relatively independent and simple and is easy to process. Furthermore, the dimension of the design is more compact

than most of the reported antennas. The measurement and simulations match well. Both the time-domain and frequency-domain characteristics of the proposed design are very good. The proposed design has good function of in-band and out-of-band filtering, and it is very suitable for UWB system.

#### 5 Acknowledgments

This work was supported in part by the National Defence Pre-Research Foundation of China (grant no. 6140450010302), Doctoral Innovation Fund of Xi'an University of Technology, Key research and development plan of Shaanxi Province (2017ZDXM-GY-117).

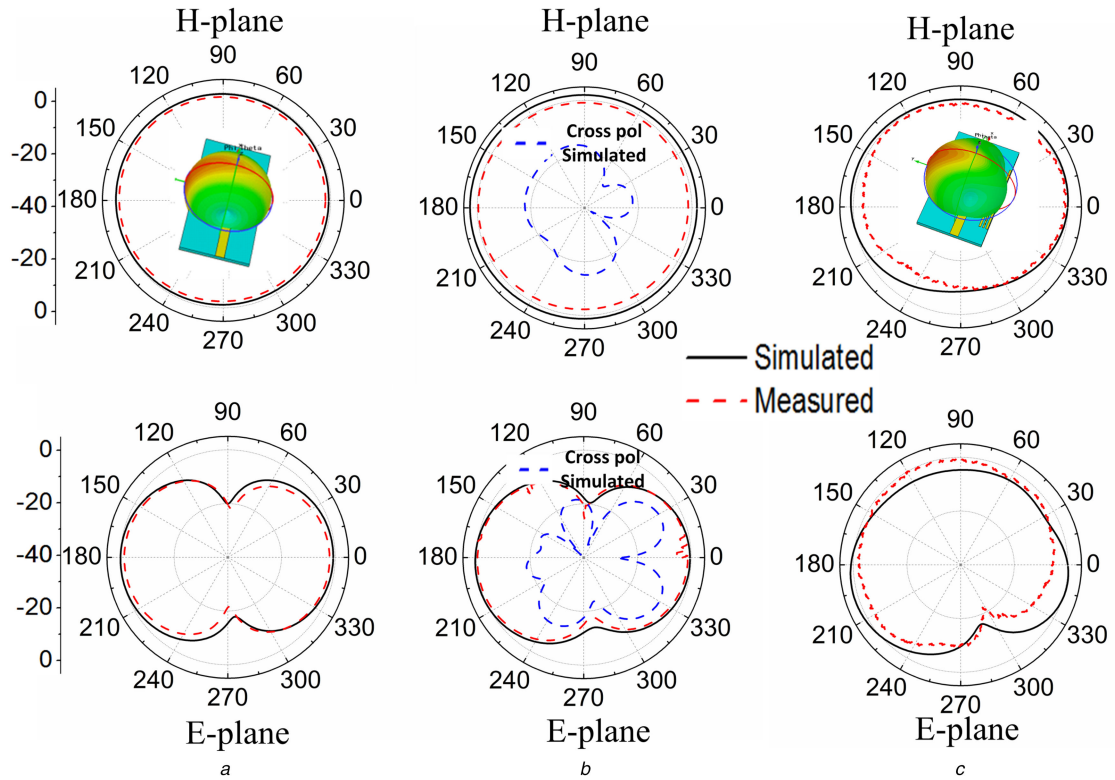


**Fig. 12** Simulated and Measured normalized radiation patterns of the proposed design in state I (a) 3.1 GHz, (b) 6 GHz, (c) 10 GHz

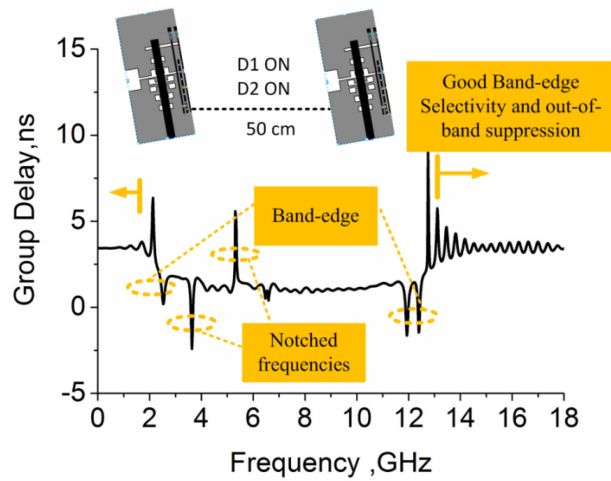


**Fig. 13** Group delay of the proposed design in state IV

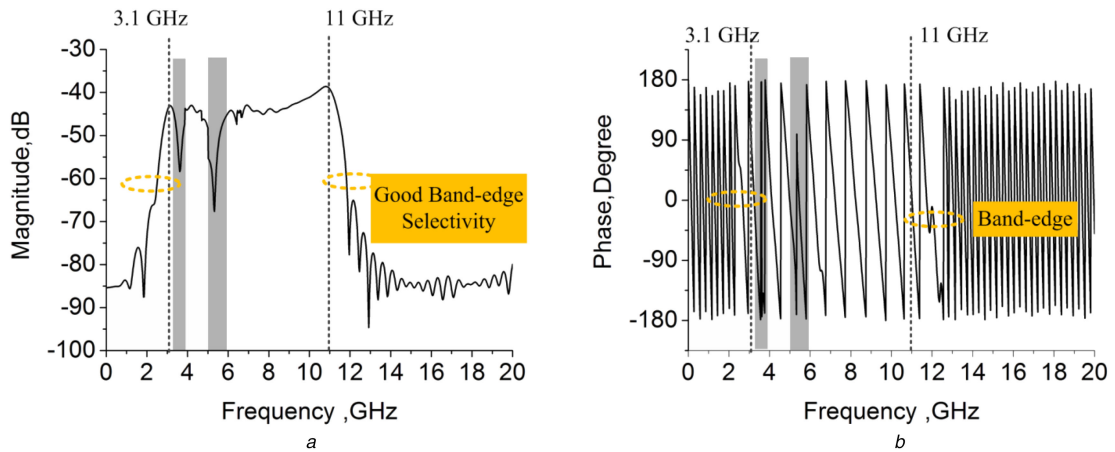


**Fig. 14** Transfer function of the proposed antenna in state IV (a) Measured magnitude, (b) Measured phase S21

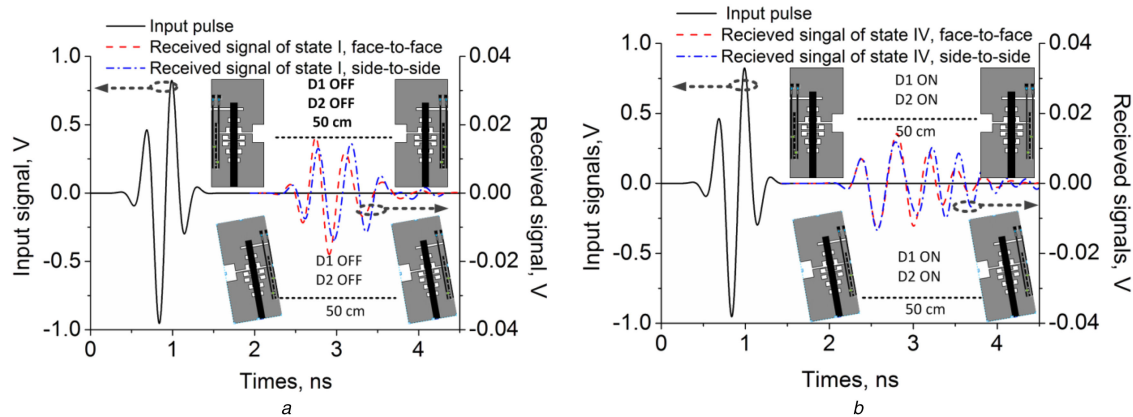


**Fig. 15** Input and received pulses in different cases of the UWB antenna in state I and state IV  
(a) State I, (b) State IV

## 6 References

- [1] Federal Communications Commission: 'First report and order, revision of part 15 of commission's rule regarding ultra-wideband transmission systems'. FCC 02-48, April 22 2002
- [2] Wu, J.N., Zhao, Z.Q., Nie, Z.P., *et al.*: 'A printed unidirectional antenna with improved upper band-edge selectivity using a parasitic loop', *IEEE Trans. Antennas Propag.*, 2015, **63**, (4), pp. 1832–1837
- [3] Wong, S.W., Huang, T.G., Mao, C.X., *et al.*: 'Planar filtering ultra-wideband (UWB) antenna with shorting pins', *IEEE Trans. Antennas Propag.*, 2013, **61**, (2), pp. 948–953
- [4] Singhal, S., Singh, A.K.: 'Asymmetrically CPW-fed ladder-shaped fractal antenna for UWB applications', *Analog Integr. Circuits Signal Process.*, 2017, **92**, (1), pp. 91–101, 2017
- [5] Manohar, M., Kshetrimayum, R.S., Gogoi, A.K.: 'A compact dual band-notched circular ring printed monopole antenna for super wideband applications', *Radioengineering*, 2017, **26**, (1), pp. 64–70
- [6] Emadian, S.R., Ahmadi-Shokouh, J.: 'Very small dual band-notched rectangular slot antenna with enhanced impedance bandwidth', *IEEE Trans. Antennas Propag.*, 2015, **63**, (10), pp. 4529–4534
- [7] Sun, Y.H., Wen, G.J., Jin, H.Y., *et al.*: 'Gain enhancement for wide bandwidth endfire antenna with I-shaped resonator (ISR) types', *Electron. Lett.*, 2013, **49**, (12), pp. 736–737
- [8] Yang, M., Yin, X.X., Chen, Z.N., *et al.*: 'Planar image-reject bow-tie antenna with gain enhancement for superheterodyne applications', *IEEE Antennas Wirel. Propag. Lett.*, 2016, **15**, pp. 658–661
- [9] Badjian, M.H., Chakrabarty, C.K., Hock, G.C., *et al.*: 'An impulse UWB patch antenna with integrated bandpass filter'. Telecommunication Technologies 2008 and 2008 2nd Malaysia Conf. on Photonics, Putrajaya, Malaysia, August 2008, pp. 166–169
- [10] Li, R., Gao, P.: 'Design of a UWB filtering antenna with defected ground type', *Progress in Electromagn. Res. Lett.*, 2016, **63**, pp. 65–70
- [11] Sahoo, A.K., Gupta, R.D., Parihar, M.S.: 'High selective integrated filter antenna for UWB application', *Microw. Opt. Technol. Lett.*, 2017, **59**, (5), pp. 1032–1037
- [12] Yang, H.L., Xi, X.L., Zhao, Y.C., *et al.*: 'Design of compact ultra-wideband slot antenna with improved band-edge selectivity', *IEEE Antennas Wirel. Propag. Lett.*, 2018, **6**, (17), pp. 946–950
- [13] Chandel, R., Gautam, A.K., Rambabu, K.: 'Tapered fed compact UWB MIMO-diversity antenna with dual band-notched characteristics', *IEEE Trans. Antennas Propag.*, 2018, **66**, (4), pp. 1677–1684
- [14] Gautam, A.K., Yadav, S., Rambabu, K.: 'Design of ultra-compact UWB antenna with band-notched characteristics for MIMO applications', *IET Microw. Antennas Propag.*, 2018, **12**, (12), pp. 1895–1900
- [15] Chen, W.X., Lee, C.H., Hsu, C.I.G.: 'CM suppression enhancement for balanced band-notched UWB closed-aperture antenna', *Electron. Lett.*, 2017, **53**, (19), pp. 1291–1292
- [16] Rehman, S.U., Alkanhal, M.A.S.: 'Design and system characterization of ultra-wideband antennas with multiple band-rejection', *IEEE Access.*, 2017, **5**, pp. 17988–17996
- [17] Li, W.T., Hei, Y.Q., Subbaraman, H., *et al.*: 'Novel printed filtenna with dual notches and good out-of-band characteristics for UWB-MIMO applications', *IEEE Micro. Wiel. Co.*, 2016, **26**, (10), pp. 765–767
- [18] Vendik, I.B., Rusakov, A., Ket, K., *et al.*: 'Ultrawideband (UWB) planar antenna with single-, dual-, and triple-band notched characteristic based on electric ring resonator', *IEEE Antennas Wirel. Propag. Lett.*, 2017, **16**, pp. 1597–1600
- [19] Yang, H.L., Xi, X.L., Zhao, Y.C., *et al.*: 'A compact filtering UWB antenna with band-notched function', *IEICE Electron. Express*, 2018, **15**, pp. 20180458–20180458
- [20] Badamchi, B., Nourinia, J., Ghobadi, C., *et al.*: 'Design of compact reconfigurable ultra-wideband slot antenna with switchable single/dual band notch functions', *IET Microwaves Antennas & Propag.*, 2014, **8**, pp. 541–548
- [21] Valizade, A., Ghobadi, C., Nourinia, J., *et al.*: 'A novel design of reconfigurable slot antenna with switchable band notch and multiresonance functions for UWB applications', *IEEE Antennas Wirel. Propag. Lett.*, 2012, **11**, pp. 1166–1169
- [22] Yang, H.L., Xi, X.L., Hou, H.L., *et al.*: 'Design of reconfigurable monopole antenna with switchable dual band-notches for UWB applications', *Int. J. Microw. Wirel. Tech.*, 2018, **10**, (9), pp. 1065–1071
- [23] Yang, H.L., Xi, X.L., Wang, L.L., *et al.*: 'Design of reconfigurable filtering ultra-wideband antenna with switchable band-notched functions', *Int. J. Microw. Wirel. Tech.*, 2018, pp. 1–8, doi: 10.1017/S1759078718001587
- [24] Srivastava, G., Mohan, A., Chakrabarty, A.: 'Compact reconfigurable UWB slot antenna for cognitive radio applications', *IEEE Antennas Wirel. Propag. Lett.*, 2017, **16**, pp. 1139–1142
- [25] Song, Y., Yang, G., Geyi, W.: 'Compact UWB bandpass filter with dual notched bands using defected ground structures', *IEEE Microw. Wirel. Components Lett.*, 2014, **24**, (4), pp. 230–232
- [26] Yang, H.L., Xi, X.L., Zhao, Y.C., *et al.*: 'Co-designed defected ground structure filter with UWB slot antenna', *IEICE Electron. Expr.*, 2018, **15**, pp. 1–10
- [27] Pozar, D.M.: '*Microwave engineering*' (John Wiley & Sons, Inc., 1998, 2nd edn.), pp. 399–425

## 西安理工大学检索收录证明

检索工具	SCI-E (科学引文索引-扩展)	版本	网络版
收录作者	杨海龙	查证人	靳秀敏
作者学院	自动化与信息工程学院	查证日期	2019-10-11

标题: Compact slot antenna with enhanced band-edge selectivity and switchable band-notched functions for UWB applications

作者: Yang, HL (Yang, Hailong); Xi, XL (Xi, Xiaoli); Zhao, YC (Zhao, Yuchen); Tan, YM (Tan, Yumeng); Yuan, YN (Yuan, Yanning); Wang, LL (Wang, Lili)

来源出版物: IET MICROWAVES ANTENNAS & PROPAGATION 卷: 13 期: 7 页: 982-990 DOI: 10.1049/iet-map.2018.5832 出版年: JUN 12 2019

入藏号: WOS:000471759500017

语言: English

文献类型: Article

作者关键词: microstrip antennas; ultra wideband antennas; impedance matching; defected ground structures; microwave antennas; antenna radiation patterns; band-pass filters; slot antennas; antenna feeds; compact slot antenna; enhanced band-edge selectivity; switchable band-notched functions; reconfigurable stepped slot; switchable band-notched characteristic; out-of-band rejection; defected ground structure; DGS; parasitic slot; good cut-off property; excellent selectivity; notched band; passive strip line; antenna radiation structure; competitive antennas; out-of-band characteristics; different UWB applications; noise figure 10; 0 dB; noise figure-3; 0 dB; frequency 3; 1 GHz to 11; 1 GHz

Key Words Plus: MONOPOLE ANTENNA; DESIGN; FILTER

地址: [Yang, Hailong; Xi, Xiaoli; Zhao, Yuchen; Tan, Yumeng; Yuan, Yanning; Wang, Lili] Xian Univ Technol, Fac Automat & Informat Engn, Xian 710048, Shaanxi, Peoples R China.

[Xi, Xiaoli] Northwest Inst Nucl Technol, Sci & Technol High Power Microwave Lab, Xian 710024, Shaanxi, Peoples R China.

通讯作者地址: Xi, XL (通讯作者), Xian Univ Technol, Fac Automat & Informat Engn, Xian 710048, Shaanxi, Peoples R China.

Xi, XL (通讯作者), Northwest Inst Nucl Technol, Sci & Technol High Power Microwave Lab, Xian 710024, Shaanxi, Peoples R China.

电子邮件地址: xixiaoli@xaut.edu.cn

出版商: INST ENGINEERING TECHNOLOGY-IET

出版商地址: MICHAEL FARADAY HOUSE SIX HILLS WAY STEVENAGE, HERTFORD SG1 2AY, ENGLAND

Web of Science 类别: Engineering, Electrical & Electronic; Telecommunications

研究方向: Engineering; Telecommunications

IDS 号: ID6AR

ISSN: 1751-8725

eISSN: 1751-8733

29 字符的来源出版物名称缩写: IET MICROW ANTENNA P

ISO 来源出版物缩写: IET Microw. Antennas Propag.

来源出版物页码计数: 9

基金资助致谢: This work was supported in part by the National Defence Pre-Research Foundation of China (grant no. 6140450010302), Doctoral Innovation Fund of Xi'an University of Technology, Key research and development plan of Shaanxi Province (2017ZDXM-GY-117).

基金资助机构: National Defence Pre-Research Foundation of China, 授权号: 6140450010302

基金资助机构: Doctoral Innovation Fund of Xi'an University of Technology, 授权号:

基金资助机构: Key research and development plan of Shaanxi Province, 授权号: 2017ZDXM-GY-117

输出日期: 2019-10-11